INVESTIGATION OF STRAIN HETEROGENEITIES BY LASER SCANNING EXTENSOMETRY IN STRAIN AGEING MATERIALS: APPLICATION TO ZIRCONIUM ALLOYS

S. Graff[a] *, H. Dierke[b], H. Neuhäuser[b], S. Forest[a], J.–L. Strudel[a], C. Prioul[c], J.–L. Béchade[d]

[a] Centre des Matériaux / UMR 7633, Ecole des Mines de Paris / CNRS,
BP 87, 91003 Evry France

[b] Institut für Physik der Kondensierten Materie,
38106 Braunschweig Germany

[c] MSSMAT, Ecole Centrale Paris, Grande Voie des Vignes, 92295 Châtenay–Malabry France

[d] SRMA, CEA Saclay, 91191 Gif sur Yvette France

Abstract: Laser scanning extensometry was used to detect and characterize propagating plastic instabilities such as the Lüders bands at the millimeter scale. Spatio–temporal plastic heterogeneities are due to either static or dynamic strain ageing (SSA and DSA) phenomena. Regarding zirconium alloys, different type of heterogeneities were observed: their features strongly depended on mechanical test conditions. In one case, they appeared to be non propagating but preserved along the stress-strain curve and were associated with SSA effects such as stress peaks after relaxation periods or after unloading steps with waiting times. In other case, they appeared as non propagating but were not associated with SSA effects.

Keywords: Dynamic strain ageing, Lüders behavior, Portevin–Le Châtelier effect, Static strain ageing, Zirconium alloys

1. Introduction

Plastic deformation in crystalline materials very often proceeds by the formation and propagation of deformation bands. Only a small part of the specimen volume is strongly active, in regions which are typically in the range of μm to *mm* wide, depending on material, mechanism and deformation conditions. A variety of such deformation

*Corresponding author. Tel.: (33) 1 60 76 30 46; fax: (33) 1 60 76 31 50.
E-mail address: stephanie.graff@mat.ensmp.fr

bands were observed in particular the Lüders bands in iron and steel at the onset of plastic deformation [?] or the Portevin–Le Châtelier effect in aluminum alloys during the deformation process [?]. More accurately, such plastic instabilities were studied by multiple zone laser scanning extensometry in polycrystalline Al–Cu15% by Casarotto and Klose [?].

In numerous zirconium alloys, a non conventional viscoplastic behavior over the temperature range of approximately $200°C$–$500°C$ were reported. The phenomena observed included for instance discontinuous plastic flow [?] and low strain rate sensitivity [?]. Many of these phenomena were related to dynamic strain ageing (DSA), and different mechanisms were proposed such as the interaction between mobile dislocations and the interstitial atoms (oxygen, carbon...). Also substitutional atoms (hafnium, tin...) played an important role in these interactions [?].

The aim of the present work is to prove if strain ageing phenomena lead to strain heterogeneities at the millimeter scale in various ziconium alloys. The type of heterogeneities are compared to the case of this of more standard alloys such as mild steels and aluminum alloys.

2. Presentation of laser scanning extensometry and materials

The experimental method selected in this work is the laser scanning extensometry technique. The specimens investigated were machined in flat geometry. The length of the specimens was 45 *mm*, the width was 4 *mm* and the thickness was 1.4 *mm*. Prior to preparation for the laser extensometry measurements, a darker base layer capable of sustaining high temperatures during deformation was deposited on the length of the specimens. Then white zones (width and distance 1 *mm*) were sprayed on this base layer. The total gage length scanned and recorded by the extensometer was 30 *mm* and was divided into 12 black and white zones (bright–dark boundaries). Fig.1 presents the specimen and the experimental set up. A rotating cubic glass prism scanned a red laser beam along the specimen across the white and black zones painted to its surface at a rotation frequency of 50 Hz. The reflected signal was focused on a photodiode and its intensity was measured. The second derivative gave the time shift between each intensity

alteration referring to the stripe structure. With the reference of the initial state and the known rotation frequency these time intervals could be converted into successive positions in space of all the identified zones. Consequently a practically simultaneous measurement of "local axial strain" could be done with this method along the whole stress–strain curve (strictly speaking, strain was averaged over the 2 *mm* width of the pair of white and black zones). The resolution of the measured displacement was 1 μm. This resulted in a precision of 0.0005. The time resolution was about 20 *ms*. What is important is that such plastic heterogeneities or local strains can be detected at the millimeter scale. The investigated volume in any identified painted cell (each pair of white and black zones) was nearly equal to 8 mm^3.

The studied materials were a mild steel and an aluminum alloy, that we would call standard alloys which were compared with two zirconium alloys:

- mild steel and Al–Cu4% alloy were the same as those used in [?]
- zirconium 702, labelled Zr702, contained 2280 *ppm* tin and 1300 *ppm* oxygen
- zirconium doped with hafnium, labelled ZrHf, contained 2.2% hafnium and 100 *ppm* oxygen.

The main difference between these two zirconium alloys was that Zr702 contained more oxygen than ZrHf. The substitutional atoms were tin and hafnium respectively in Zr702 and ZrHf.

For all the tensile tests, a stiff tensile machine was used, which was "softened" by an additional spring within the horizontal tensile axis. This tensile machine was built by Neuhäuser and Traub [?]. The load was transmitted to the tensile rod via a ball bearing spindle to reduce friction. The heating of the specimen up to maximum temperature of about 300°*C* could be obtained.

3. Results

3.1. Detection of Lüders bands in mild steel and application to DSA in Al–Cu4% alloy

First, in order to validate the experimental set up of the laser scanning extensometry used for measurements of plastic heterogeneities at the millimeter scale, standard alloys were

tested.

The first plastic instability is the Lüders band observed in mild steel at room temperature. The strain rate of the tensile test was $8.10^{-4}s^{-1}$. The tensile test was carried out with fifteen minutes relaxation periods. Fig.2 shows the macroscopic tensile curve and also the local strain detected by the laser scanning extensometer as a function of the position on the specimen for various strain levels (or the 2 *mm* width of the pair of white and black zones). The mechanism of the Lüders behavior is the dislocation locking, resulting from an ageing process. An important stress is necessary to unlock the dislocations, which is equal to 262 MPa ("upper yield stress"). Then it is easier to create other fresh dislocations for instance at the grips. They can also move easily and a strain band labelled "Lüders band" appears, whose length of 0.03 strain, and propagates at a stress level inferior to the upper yield stress ("lower yield stress"), equal to 247 MPa. Consequently a stress peak appears on the macroscopic curve of Fig.2, which is followed by the Lüders band, moving into the entire specimen. Afterwards, the plastic deformation goes on homogeneously following a classic work hardening stress–strain path. An other view of the propagation of the Lüders band front can be observed on the the local strain–position curve inserted in Fig.2, which can illustrate the propagation mode during straining. We can follow the initiation of the Lüders band at one grip of the specimen and its propagation along the axis of the specimen at various strain levels. It is obviously clear that the Lüders band contains 0.003 strain.

An other plastic instability is the Portevin–Le Châtelier effect (or PLC bands) observed in Al–Mg3% at room temperature. This jerky flow was studied in detail by Ziegenbein, Klose and al. [?, ?]. Fig.3 shows the macroscopic tensile curve and also the local strain detected by the laser scanning extensometer as a function of the position on the specimen for different strain levels. The serrations observed on the overall tensile curve of Fig.3 and associated with PLC effects are classically labeled as types A, B and C according to [?]. Type A appears as a continuous propagation of PLC bands, which are usually nucleated with a slight yield point near one specimen grip and propagate with a nearly constant velocity and band width to the other end of the specimen. These bands sweep across the gauge length periodically. The increase in strain is quite slow and the fluctuations of load are moderate during propagation. The external applied strain (rate) is concentrated within the active width of the PLC band and the rest of the specimen contributes hardly any additional strain (rate). Type B bands propagate discontinuously along the specimen,

or more precise, small strain bands nucleate in the nearest surroundings of the former band. Type C PLC deformation is characterized by spatially random nucleation of bands without subsequent propagation accompagnied by strong, high frequency and regular load drops.

On the local strain–position curve inserted in Fig.3, serrations type B, which are not so easily to recognize on the macroscopic tensile curve, can be clearly proved. For instance, by comparison with 0.035 and 0.07 strain levels, the zones 7 and 10 are affected by PLC effects: small strain bands propagate into these two strongly deformed zones. Also at 0.07 and 0.12 strain levels, the zones 11 and 15 are affected by localized strain bands which can propagate at short distance.

Fig.4 represents the macroscopic curves of two tensile tests realized at a constant strain rate of $8.10^{-4}s^{-1}$ and $8.10^{-5}s^{-1}$ respectively for Al–Cu4% alloy at room temperature. During each tensile tests, some relaxation periods of fifteen minutes at different strain levels were carried out in order to detect the existence of stress peaks due to static strain ageing (SSA) during the hold time. The main observation is that this material exhibits an inverse strain rate sensibility behavior because the macroscopic curve at $8.10^{-5}s^{-1}$ is above this at $8.10^{-4}s^{-1}$, which is due to the strain ageing phenomena (diffusive process od solute atoms around the mobile dislocation). The stress peaks observed after each relaxation periods are all the more pronounced that the strain rate is small. Yet the local strain as a function of the position is found to be homogeneous: the value of the local strain heterogeneities detected at various strain levels are smaller than the resolution in strain.

3.2. Strain ageing phenomena in several zirconium alloys

Various non conventional behaviors were observed in different zirconium alloys during the thirty years:

- the lowering of the strain rate sensitivity in Zircaloy–4 [?]
- the Lüders band formation in zirconium 1%Nb [?]
- the interruption of the creep in zirconium 702 [?]...

All these effects, associated with the dynamic strain ageing, were observed in the temperature range $200°C$–$500°C$ and for specific imposed strain rates. For such materials exhibiting strain ageing phenomena, the question is to know whether strain

heterogeneities exist or not at the millimeter scale. The aim of this work is also to characterize the type of strain heterogeneities by comparison with standard materials presented in the last section.

The first zirconium alloy tested is the zirconium 702 (Zr702). This material exhibits an inverse strain rate sensitivity at $300°C$ as shown in Fig.5 where the macroscopic curves of two tensile tests realized at constant strain rates of $10^{-4}s^{-1}$ and $10^{-5}s^{-1}$ respectively are presented. This effect is usually attributed to the dynamic strain ageing phenemena due to the interaction between the oxygen atoms and the mobile dislocations in this case [?]. Tensile tests at a constant strain rate of $8.10^{-5}s^{-1}$ with relaxation periods of fifteen minutes were realized for the temperatures $20°C$, $100°C$ and $250°C$. Because of the tensile machine was stiff enough, the strain could not be maintained exactly constant during the relaxation periods. The macroscopic curves of Fig.6 show that the Zr702 exhibits SSA only at $250°C$. The stress peaks after relaxation periods are rather bulge. For the same various strain levels at $20°C$ and $250°C$, the local strains were measured and plotted as a function of the position in Fig.7(a) at $20°C$ and in Fig.7(b) at $250°C$. A conventional behavior associated with an homogeneous response is observed for different strain levels at $20°C$. However at $250°C$, strain heterogeneities are observed at the millimeter scale. Initially for small deformations, for instance at 0.006 strain level, strain heterogeneities are present in all the zones. During straining these heterogeneities are non propagating. Comparing with mild steel and Al–Mg3% allooy, this type of strain heterogeneity is not a propagating one like the Lüders band and is not a PLC instability. Ferrer and al. showed in a zirconium alloy labelled M5 that for small deformations (about 0.02 strain level), after a tensile test carried out at a constant strain rate of $5.10^{-5}s^{-1}$ at $200°C$, that glide ligns were not observed in all the grains: the strain was localized in some specific grains. However, regarding the local strain measurements, all the zones are affected by straining. Such a difference can be explained by the scale level which is not the same between the two studies.

An other mechanical tests are now considered namely tensile tests with partial unloading steps and waiting times. Fig.8 shows the macroscopic curves obtained at an imposed strain rate $8.10^{-5}s^{-1}$ at $20°C$ and $250°C$. Static strain ageing is observed only at $250°C$ and the stress bulges are similar to those observed in Fig.6. The stress peak is more pronounced at the first partial unloading because the waiting time is equal to 24 hours

contrary to the other partial unloadings with hold times of just a few minutes. The curves which represent the local strain as a function of the position for different strain levels on Fig.8 are those obtained at $20°C$. Even though there is no SSA effect on the macroscopic curve, strain heterogeneities are observedat the millimeter scale. Moreover, for small deformations, for instance at 0.007 strain level, strain heterogeneities are observed like for the tensile test with relaxations. They are of the same type as those found during the tensile test with relaxations at $250°C$. Such heterogeneities are also observed at $250°C$ where SSA occurs. The amplitude of strain heterogeneities can reach 0.015.

For comparison, we tested other zirconium alloy, the zirconium alloy doped with hafnium (ZrHf). The same mechanical tests as the previous one were performed in the same experimental conditions. Regarding the tensile tests with partial unloading steps and waiting times at $8.10^{-5}s^{-1}$ at $20°C$ and $250°C$, Fig.9 shows that ZrHf exhibits a SSA effect which is characterized by an increase of the stress after each unloading steps at $250°C$. This is similar to Zr702. At the beginning of straining, no strain heterogeneities are measured up to 0.02 strain level, contrary to Zr702 in which initial heterogeneities are observed at the beginning of straining (see Fig.8). Then the strain heterogeneities are no propagating.

Fig.10 shows the macroscopic curves obtained during the tensile tests with relaxation periods realized at a constant strain rate of $8.10^{-5}s^{-1}$ at $20°C$ and $100°C$. There is no strain ageing after relaxation periods as observed in Zr702 (see Fig.6). As the tensile tests with partial unloading steps and waiting times, the strain level for which strain heterogeneities are measured id 0.016, contrary to Zr702 for which initial heterogeneities are observed at the beginning of straining (see Fig.7(b)). This is the main difference between the two zirconium alloys studied. One can argue that the oxygen atoms can favor the initial heterogeneities for the Zr702. As in Zr702 and for tensile tests with partial unloading steps and waiting times, the type of heterogeneity is the same: the instabilities are no propagating.

4. Concluding discussion and perspective

Laser scanning extensometry is an appropriate method to identify and characterizes plastic heterogeneities at the millimeter scale.

Table 1 gives the classification of SSA and DSA phenomena during tensile tests carried out at a constant strain rate for standard materials such as mild steel, Al–Mg3% and Al–Cu4%. Table 2 and Table 3 give the classification of SSA and DSA phenomena during tensile tests carried out at a constant strain rate respectively including relaxation periods and with unloading steps and waiting times for zirconium alloys.

Taking into account these observations and the results of the local strain as a function of position curves, we can suggest the following classification of strain heterogeneities:

1. Lüders band: continuous propagation of strain band front moving over the entire specimen only once and with a nearly constant velocity (for example mild steel)
    - PLC type A bands: strain bands usually propagative continuously with a nearly constant velocity and band width. They reach the other end of the specimen and are reflected. PLC bands sweep across the gauge length periodically.
    - PLC type B bands: small strain bands nucleate, propagate and vanish at random in various regions of the specimen (for example Al–Mg3% alloy)
    - PLC type C bands: spatially random nucleation of stain bursts with short life time and without significant propagation
2. no plastic heterogeneities but SSA effect such as stress peaks after relaxation periods (for example Al–Cu4% alloy)
3. non propagating strain heterogeneities associated with SSA effects such as stress peaks after relaxation periods or unloading steps with waiting times (for example Zr702 and ZrHf at $250°C$)
4. non propagating strain heterogeneities associated with no SSA effects (for example Zr702 and ZrHf at $100°C$)

As complex strain localization phenomena take place in the zirconium alloys, it should be interesting to make some investigations at the sub–millimeter scale: How do plastic heterogeneities initiate? What is the role of the interstitial atoms like oxygen atoms? How are they preserved when strain increases?

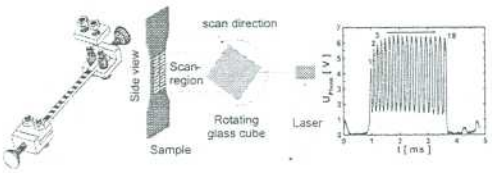
scan direction
Side view
Scan-region
Rotating glass cube
Laser
Sample
t [ms]

Fig.1

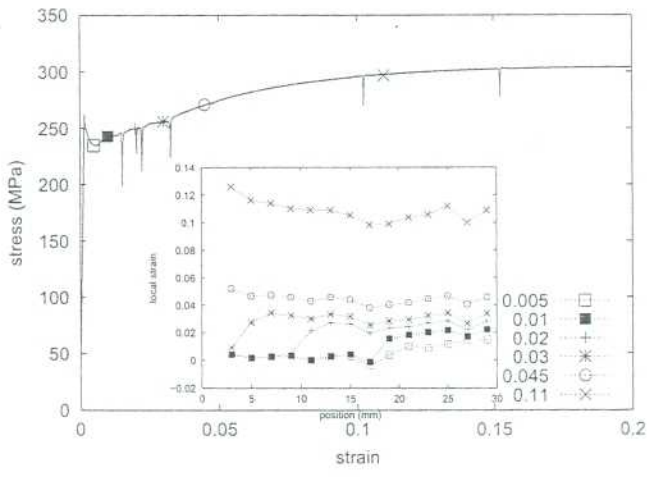
stress (MPa)
strain
local strain
position (mm)
0.005
0.01
0.02
0.03
0.045
0.11

Fig.2

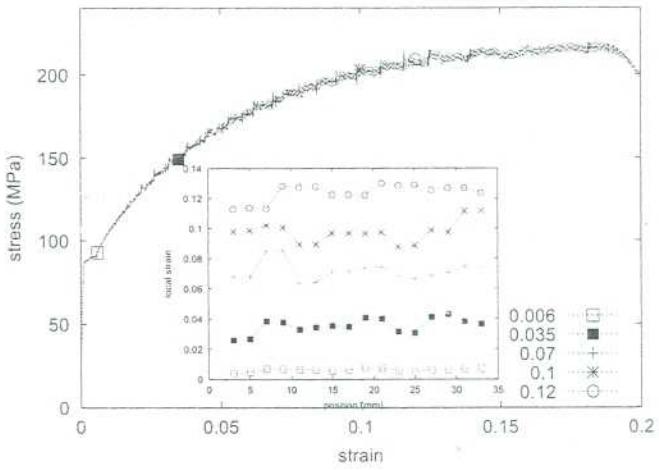
stress (MPa)
strain
0.006
0.035
0.07
0.1
0.12

Fig.3

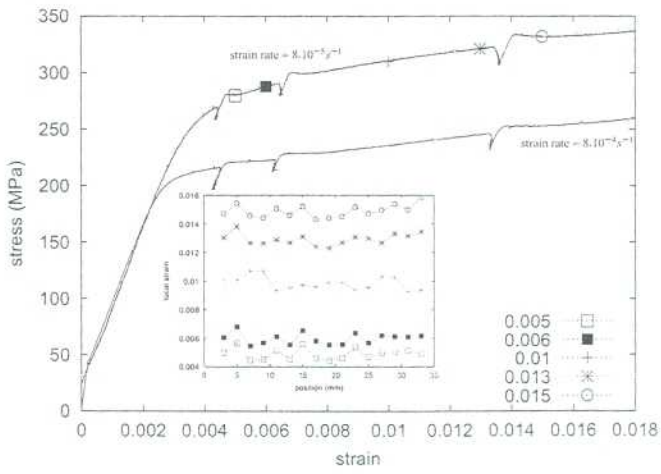
stress (MPa)
strain
0.005
0.006
0.01
0.013
0.015

Fig.4

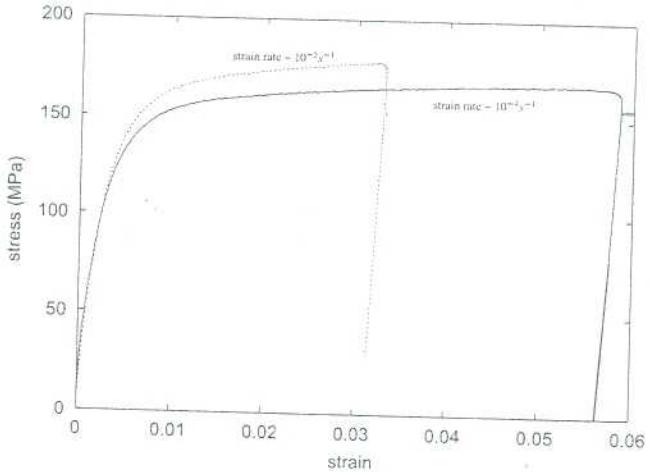
200
150
100
50
0
stress (MPa)
0
0.01
0.02
0.03
0.04
0.05
0.06
strain

Fig.5

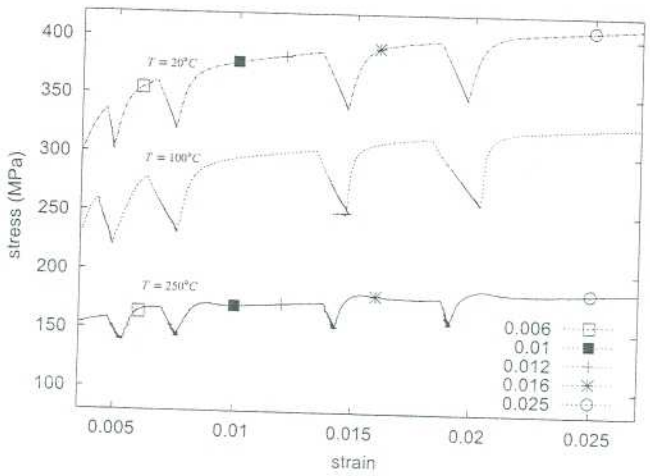
400
350
300
250
200
150
100
stress (MPa)
T = 20°C
T = 100°C
T = 250°C
0.006
0.01
0.012
0.016
0.025
0.005
0.01
0.015
0.02
0.025
strain

Fig.6

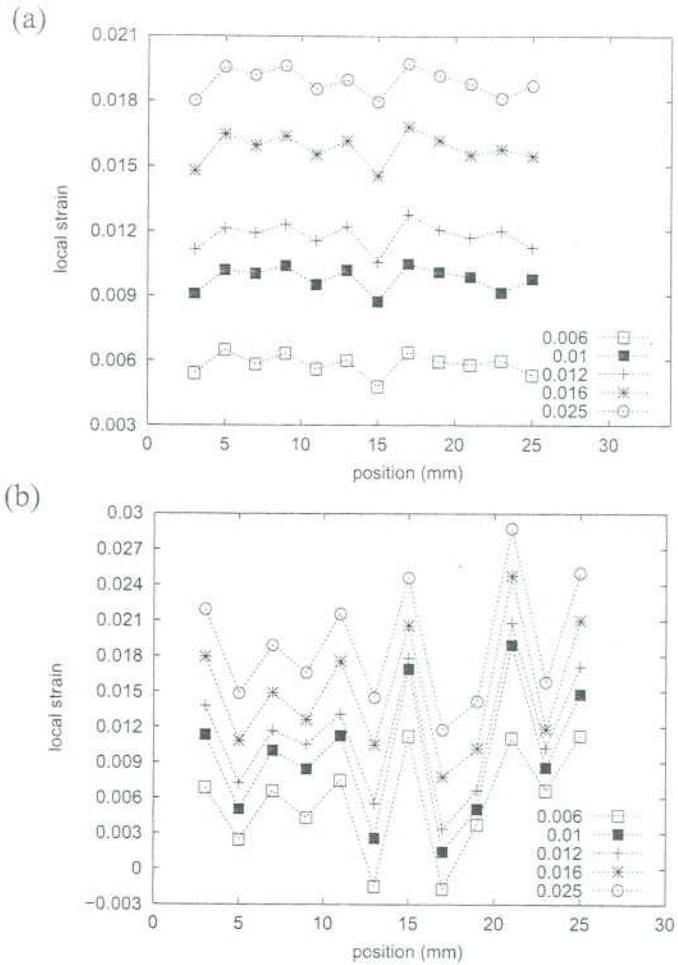

Fig.7(a) and Fig.7(b)

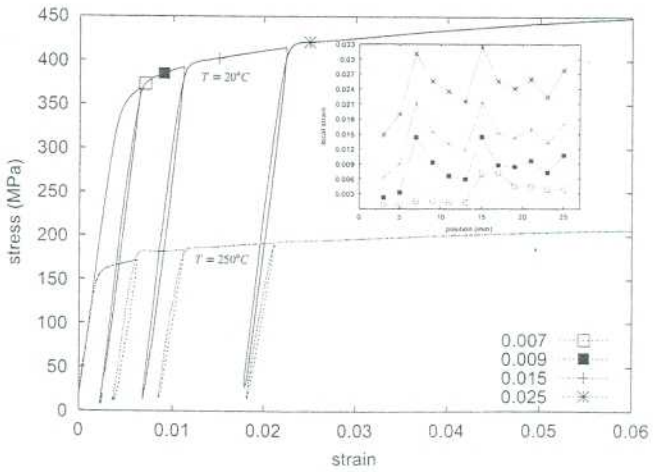

Fig.8

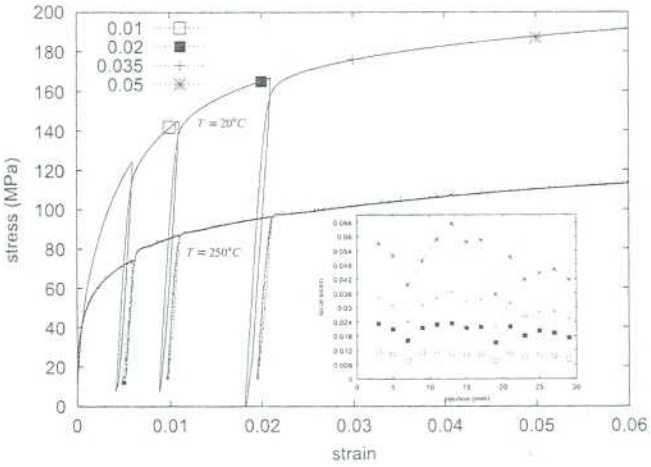
0.01
0.02
0.035
0.05
T = 20°C
T = 250°C
stress (MPa)
strain
0
20
40
60
80
100
120
140
160
180
200
0.01
0.02
0.03
0.04
0.05
0.06

Fig.9

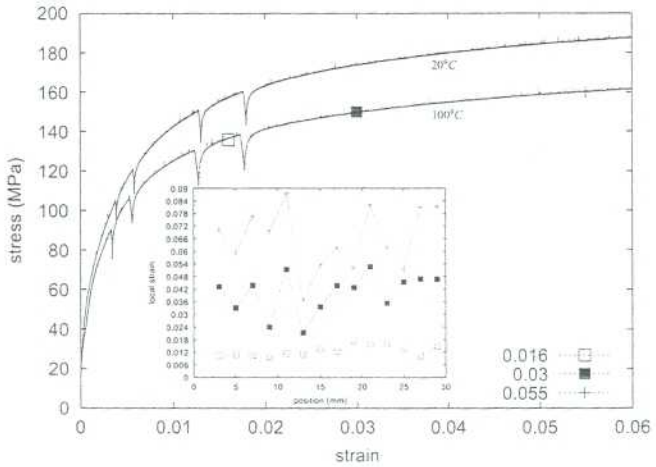
20°C
100°C
0.016
0.03
0.055
stress (MPa)
strain
0
20
40
60
80
100
120
140
160
180
200
0.01
0.02
0.03
0.04
0.05
0.06

Fig.10

Fig.1: Picture of prepared sample–Schematic of the laser scanning extensometer–Voltage of the photodiode which is proportional to the reflected intensity for 18 zones

Fig.2: Macroscopic stress-strain curve at room temperature for mild steel obtained during tensile test at a constant strain rate of $8.10^{-4}s^{-1}$; Local strain vs position curves for various strain levels selected and identified on the macroscopic curve

Fig.3: Macroscopic stress-strain curve at room temperature for Al–Mg3% obtained during tensile test at a constant strain rate of $10^{-4}s^{-1}$; Local strain vs position curves for for various strain levels selected and identified on the macroscopic curve

Fig.4: Macroscopic curves stress-strain curve at room temperature for Al–Cu4% obtained during tensile tests at a constant strain rate of $8.10^{-5}s^{-1}$ and $8.10^{-4}s^{-1}$ interrupted by fifteen minutes relaxation periods; Local strain vs position curves for various strain levels marked on the macroscopic curve

Fig.5: Inverse strain rate sensitivity exhibited by zirconium 702 at $300°C$

Fig.6: Macroscopic stress-strain curves at $20°C$, $100°C$ and $250°C$ for zirconium 702 obtained during tensile tests at a constant strain rate of $8.10^{-5}s^{-1}$ interrupted by fifteen minutes relaxation periods

Fig.7: Local strain vs position curves for zirconium 702 corresponding to the tensile test at a constant strain rate of $8.10^{-5}s^{-1}$ for various strain levels marked on the macroscopic curve (see Fig.5) at $20°C$ (a) and at $250°C$ (b)

Fig.8: Macroscopic stress-strain curves at $20°C$ and $250°C$ for zirconium 702 obtained during tensile tests at a constant strain rate of $8.10^{-5}s^{-1}$ interupted with unloading steps and waiting times ; Local strain vs position curve at $20°C$ for various strain levels shown on the macroscopic curve

Fig.9: Macroscopic stress-strain curves at $20°C$ for zirconium alloy doped with hafnium obtained during tensile tests with unloading steps and waiting times; Local strain

vs position curves for various strain levels marked on the macroscopic curve

Fig.10: Macroscopic stress–strain curves at $20°C$ and $150°C$for zirconium alloy doped with hafnium obtained during tensile tests at a constant strain rate of $8.10^{-5}s^{-1}$ interrupted with relaxation periods; Local strain vs position curves for various strain levels marked on the macroscopic curve

Table 1: Classification of SSA and DSA phenomena during tensile tests carried out at constant strain rate for standard materials

Materials	Temperature ($°C$)	Strain rate s^{-1}	SSA	DSA	Strain heterogeneities
Mild steel	20	8.10^{-4}	upper yield stress, lower yield stress, Lüders band	no	yes
Al–Mg3%	20	10^{-4}	Lüders band	PLC serrations	yes
Al–Cu4%	20	8.10^{-5}	stress peaks after relaxation periods	inverse strain rate sensitivity	no
Al–Cu4%	20	8.10^{-4}	stress peaks after relaxation periods	inverse strain rate sensitivity	no

Table 2: Classification of SSA and DSA phenomena during tensile tests carried out at constant strain rate with relaxation periods for zirconium alloys

Materials	Temperature ($°C$)	Strain rate s^{-1}	SSA	DSA	Strain heterogeneities
Zr702	20	8.10^{-5}	no	no	no
Zr702	100	8.10^{-5}	no	no	yes
Zr702	250	8.10^{-5}	stress peaks after relaxation periods	no	yes
ZrHf	20	8.10^{-5}	no	no	no
ZrHf	100	8.10^{-5}	no	no	yes
ZrHf	250	8.10^{-5}	stress peaks after relaxation periods	no	yes

Table 3: Classification of SSA and DSA phenomena during tensile tests carried out at constant strain rate with unloading steps and waiting times for zirconium alloys

Materials	Temperature ($°C$)	Strain rate s^{-1}	SSA	DSA	Strain heterogeneitie
Zr702	20	8.10^{-5}	no	no	yes
Zr702	100	8.10^{-5}	no	no	yes
Zr702	250	8.10^{-5}	stress peaks after unloading steps and waiting times	no	yes
ZrHf	20	8.10^{-5}	no	no	yes
ZrHf	100	8.10^{-5}	no	no	yes
ZrHf	250	8.10^{-5}	stress peaks after unloading steps and waiting times	no	yes